Appendix D

Session IV

NATO Perspectives on Biological Indicators of Radiation Exposure

Govert P. van der Schans
TNO Prins Maurits Laboratory
Department of Pharmacology
Rijswijk, Netherlands

Assessment of the applicability and accuracy of biological changes induced by ionizing radiation to determine which (alone or in combination) will quickly provide the best evaluation of actual damage sustained by individuals will enable medical officers to choose the most appropriate treatment at the earliest time. This ability will enhance recovery, operational effectiveness, and survivability. This assessment has been the focus of the Biological/ Clinical Indicators Subgroup of NATO RSG.23/ Panel VIII.

An overview of biological and biophysical techniques to assess radiation exposure has recently been published by Greenstock and Trivedi [1] and is discussed elsewhere. The NATO subgroup's program examines the developments of several indicators. It should be noted that parameters which have been under study previously, and which might be useful as biological indicators are not applied any longer (e.g., monoamineoxidase activity decrease in serum, prostaglandin release (urine), volatile exhaled hydrocarbons, and histamine release).

Research on biological indicators has been concentrated on whole-body irradiation and partial-body (heterogeneous) irradiation. For whole-body irradiation, the hematological parameters include: a) changes in cell populations, b) effect of dextran sulfate, and c) immune cell abnormalities. The cytological parameters include: a) micronuclei, chromosomal aberrations (dicentrics), and b) extra chromosomal breaks as detected after premature chromosome condensation. The detection of DNA damage after whole-body irradiation has involved the immunochemical detection of radiation-induced DNA breaks in peripheral white blood cells.

The biological indicator to determine partial-body (heterogeneous) irradiation has relied on the dose-dependent decrease in the nuclear area in skin keratinocytes.

Whole-Body Irradiation

Dextran Sulfate Mobilized Reserve Cells. Biological dosimetry can be based on the decrease in the capacity of dextran sulfate to mobilize reserve cells in the peripheral blood. So far these observations have been made only in mice. Human reserve cells can also be mobilized by dextran sulfate. A radiation dose dependence in humans has not been studied as yet.

Immunological-Sensitivity Score. Combining the decrease of subsets of B-lymphocytes and T-suppressor cells post-irradiation, and comparing this to the respiratory burst response before irradiation, will indicate individual radiobiological response to irradiation and eventual outcome (prognosis).

Micronucleus System. The micronucleus system shows promise. Practical application on a large number of samples within a short time frame (hours) is problematic. Literature data indicate that micronuclei in white blood cells show a large inter- and intra-individual variation in both background levels and radiosensitivity. This results in the problematic detection of radiation doses smaller than 0.2 Gy, and an uncertainty in the detection of a radiation dose of at least 40%. Recent results suggest that at least in cultured exponentially growing cells, the sum of the number of cells containing micronuclei *plus* the number of apoptotic cells is a better parameter for

determining radiation dose than counting micronuclei alone.

Detection of DNA Damage. Currently, the immunochemical detection of DNA damage appears to be a method that can be applied under simple conditions, provided the required instruments are present [2]. It is a simple, fast immunochemical assay which can be carried out on whole blood and gives results concerning radiation dose within 1.5 hours after blood sampling (finger puncture or arm puncture). In addition, several samples can be analyzed simultaneously. A dose-dependent increase of single-strandedness in the DNA of irradiated human white blood cells (*in vivo* and *in vitro*) is observed. Immediately after irradiation, 0.2 Gy is the lower detection limit. As a result of fast repair, 1 hour after exposure the lower detection limit will be about 2 Gy. Analysis can be carried out for up to 6 hours after exposure if blood is collected in a repair inhibiting solution at ambient temperature within 1 hour after exposure.

In an intercomparison dosimetry project also intended for calibration of physical dosimeters, this biological method was tested after blood was exposed in a realistic radiation field. Moreover, the assay can be set up quickly and carried out successfully in a more simple environment. For the further validation of this method, inter- and intra-individual variation still has to be studied, both after *in vitro* and *in vivo* irradiation of human blood.

Chromosomal Aberrations. Cytological dosimetry appeared to be a valuable supplement to physical dosimetry in the case of inadvertent radiation exposures. Cytological analysis of peripheral blood lymphocytes is preferred since these have the advantage of being easily obtainable and changes induced by irradiation are of the chromosome type, involving both chromatids equally. Structural chromosomal aberrations are induced *in vitro* and *in vivo* to approximately the same extent; therefore, reference dose-effect calibration curves can be easily examined for different radiation qualities. The induced aberrations can be examined for a long time after radiation exposure since the half-life of the blood lymphocytes is approximately 3 years. Inter-individual variations in the background levels of unexposed samples render estimates below 0.05 Gy almost unattainable with any realistic degree of reproducibility. The main difficulty in using aberrations is the great labor needed to get reasonable confidence limits on the results. In addition, data are available only 2–3 days after blood sampling. Important progress has been made making use of premature chromosome condensation [3], hybridization probes and automation, i.e., making use of a metaphase-finder. Nevertheless, analysis of more than five samples a day is still problematic.

Partial-Body (Heterogeneous) Irradiation

A dose-dependent decrease of nuclear area (1-6 Gy) in human skin was observed at 24 hours both after *in vivo* and after *ex vivo* exposure. The same results were obtained after *in vivo* exposure of primate skin. This procedure is time consuming but can be conducted in a routine laboratory if the apparatus is present.

Combined Injuries, i.e., Irradiation With Other Injuries (e.g., Burns, Wounds)

Combined injuries represent a significant complication that must also be considered to achieve an accurate assessment of injury. Because biological indicators of radiation alone are still being developed, the presence of other injuries and stressors are complicating factors which remain to be studied.

Collaboration Between Dosimetrists and Biologists

Research collaboration between dosimetrists and biologists is indispensable to successfully establish and predict the value of measured doses. The objective is to determine quantitative links between physical dosimetry and specific biological damage which in turn determines an individual's acute or late

radiobiological response. It could be demonstrated that DNA damage in irradiated blood samples can correlate with physical dose both for neutron and gamma irradiations. This could also be demonstrated with respect to the induction of micronuclei and chromosomal aberrations.

Conclusions and Recommendations

For medical assessment, medical staff use various clinical indicators for determining the severity of injury both from radiation and other sources. Advice on these assessments, particularly for the radiation-exposure patient with other injuries and especially burns, is required. It is important to achieve a high degree of automation with multi-parametric analysis in any biological "dosimetry" system. This high degree of automation has been met in the development of the immunochemical assay for the detection of DNA damage, leading to much progress in the measurement of chromosomal aberrations.

The validation of the developed methods and their application for determining radiation exposure under field conditions has been an important goal, now realized. This would not have been possible without the cooperation and pooling of resources of the participating NATO defense laboratories.

Currently, there is no biological indicator available which can accurately detect low-level radiation exposure in personnel (between 0.05–70 cGy). As can be derived from mutation-induction-studies, an accumulated dose of only 0.05 Gy will result in a 25% increase of single-exon deletions. To detect this increase, single-exon deletion mutants must be detectable in an environment of 10^6 unmodified cells.

A modified PCR-amplification method in which the DNA fragment containing the deletion is amplified may provide the required sensitivity. In preliminary experiments we could already detect plasmids containing a 160-bp deletion among a 10^6-fold extent of plasmids not containing the deletion.

References

1. Greenstock CL, Trivedi A (1994) Biological and biophysical techniques to assess radiation exposure: a perspective. Prog Biophys Molec Biol 61: 81-130

2. Timmerman AJ, Mars-Groenendijk RH, van der Schans GP, Baan RA (1995) A modified immunochemical assay for the fast detection of DNA damage in human white blood cells. Mutation Res. 334:347-356

3. Blakely WF, Prasanna PGS, Kolanko CJ, Pyle MD, Mosbrook DM, Loats AS, Rippeon TL, Loats H (1995) Application of the premature chromosome condensation assay in simulated partial-body radiation exposures: evaluation of the use of an automated metaphase-finder. Stem Cells 13(1):223-230

Radiation-Induced Apoptosis in Human Lymphocytes

D.R. Boreham, K.L. Gale, S.R. Maves, D.P. Morrison, B.P. Smith, J.A. Walker, S.P. Cregan, and R.E.J. Mitchel
AECL, Chalk River Laboratories
Chalk River, Ontario, Canada

Abstract

Experimental evidence indicates that radiation-induced apoptosis in human lymphocytes has the kinetics, sensitivity, and reproducibility to be a potential biological dosimeter. Human lymphocytes were irradiated in culture and two assays were used to measure the frequency of radiation-induced apoptosis: *in situ* terminal deoxynucleotidyl transferase (TdT) assay and fluorescence analysis of DNA unwinding (FADU) assay. Induction of apoptosis in lymphocytes irradiated *in vitro* was proportional to dose and could be detected following exposures as low as 0.05 Gy. Lymphocytes from individual donors had reproducible dose responses. There was, however, variation between donors. A prior exposure of lymphocytes to small doses of

radiation sensitized cells to a subsequent radiation exposure. Hyperthermia initially sensitized then conferred resistance to radiation-induced apoptosis in lymphocytes.

The *in vivo* rate of appearance and longevity of radiation-induced apoptosis in human lymphocytes is unknown. We have determined, however, that mouse lymphocytes irradiated *in vivo* have a similar response to human lymphocytes irradiated *in vitro*. Apoptosis in mouse lymphocytes was measured using the comet assay. It was determined that samples could be incubated either as isolated lymphocytes or as whole blood. Preliminary data showed that apoptosis in lymphocytes could be measured after whole body irradiation of mice. Radiation-induced apoptosis was detectable provided lymphocytes were removed from the body within 1 hour postirradiation. Apoptosis was not detectable when lymphocytes were collected 24 hours postirradiation.

In summary, *in vitro* studies with human lymphocytes showed that radiation-induced apoptosis in lymphocytes was detectable at low doses, reproducible for individual donors, varied between individuals, and was modified by prior exposures to radiation and heat. *In vivo* studies with mice indicated that lymphocyte samples should be collected soon after whole body irradiation. In conclusion, we suggest that apoptosis in lymphocytes may be used to assess individual sensitivity to radiation and predict the biological consequences of a radiation exposure.

Introduction

In biological dosimetry it is difficult to measure the biological damage and the subsequent risks associated with radiation exposure. Chromosome aberrations and micronucleus formation are classic biological endpoints that have been used to assess radiation damage to a cell. Alternatively, we present new evidence indicating that death of white blood cells (apoptosis) may also be a useful biological indicator of radiation exposure.

Apoptosis is a form of cell death with distinctive morphological and biochemical characteristics. Fragmentation of nuclear DNA is one of the biochemical events that occurs in apoptotic cells and distinguishes them from other cells and other modes of cell death.We have used three assays to measure radiation-induced apoptosis in peripheral blood lymphocytes from humans and mice: the *in situ* Terminal Deoxynucleotidyl Transferase (TdT) assay, Fluorescence Analysis of DNA Unwinding (FADU), and the comet assay. Here we report evidence that supports the idea that apoptosis of irradiated lymphocytes has potential as a short-term biological dosimeter, appropriate for accident scenarios, and also may be useful to assess individual radiosensitivity.

Methods

Human Cell Culture and Irradiation. Blood samples were collected from healthy male volunteers in heparinized tubes. Lymphocytes were isolated, washed in Hank's Solution, and were resuspended at 4.0×10^5 cells/ml in complete growth medium. Cells were irradiated at 37°C in culture medium with either x-rays or ^{60}Co γ-rays. The two assays used to measure DNA fragmentation associated with apoptosis in human cells were TdT and FADU [1,2].

Mouse Cell Culture and Irradiation. Male CBA mice were given 1.5 Gy whole body ^{60}Co γ-rays. Blood samples (10–20 µl) were obtained by orbital bleed or tail puncture. The blood was immediately diluted in 10X complete RPMI media and sealed in a sterile 1 ml Eppendorf tube. The tube was incubated for 24 hours and then assayed for apoptosis using the comet assay [3].

Results

***Human Lymphocytes Irradiated* In Vitro.** Human lymphocytes undergo radiation-induced apoptosis in a time- and dose-dependent manner. Apoptotic cells were detectable after 6 hours of incubation following a 10-Gy exposure (fig. 1A). At 24 hours of incubation doses as low as 1.0 Gy could be detected above control levels (fig.1B). Radiation-induced apoptosis seemed to show a linear response up to 10 Gy (fig. 1B).

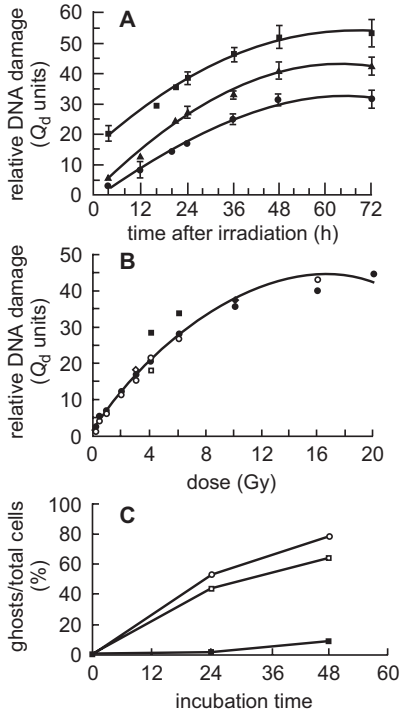

Fig. 1. (A) Time dependent appearence of apoptotic human lymphocytes following *in vitro* exposure to 3 (●), 6 (▲), and 10 (■) Gy of ^{60}Co γ-rays. (B) Dose response for radiation-induced apoptosis in human lymphocytes measured 24 hours after *in vitro* exposure. Different symbols represent data from different donors. Closed symbols indicate the same individual from repeat experiments. (C) Time dependent appearence of apoptotic mouse lymphocytes following *in vivo* irradiation (1.5 Gy ^{60}Co γ-rays) and 24 hours *in vitro* incubation (control mice [●,■], and irradiated mice [o,□]).

***Mouse Lymphocytes Irradiated* In Vivo *and Incubated* In Vitro.** Apoptotic lymphocytes could be detected in whole blood samples after 24 hours of incubation, provided the blood was removed from the mouse within 1 hour postirradiation (fig. 1C). Apoptosis was not detectable in lymphocytes from blood samples taken 24 hours postirradiation (data not shown).

Conclusions

In conclusion, *in vitro* studies with human lymphocytes showed that radiation-induced apoptosis in lymphocytes was detectable at low doses, reproducible for individual donors, varied between individuals, and was modified by prior exposures to radiation and heat. *In vivo* studies with mice indicated that lymphocyte samples should be collected soon after whole body irradiation. We propose that apoptosis in lymphocytes may be used to assess individual sensitivity to radiation and may predict the biological consequences of a radiation exposure.

Acknowledgement

This work was supported by the CANDU Owners Group.

References

1. Cregan SP, Boreham DR, Walker PR, Brown DL, Mitchel REJ (1994) Modification of radiation-induced apoptosis in radiation- or hyperthermia-adapted human lymphocytes. Biochemistry and Cell Biology 72(11-12): 475-482

2. Boreham DR, Gale KL, Maves SR, Walker J-A, Morrison DP (1996) Radiation-induced apoptosis in human lymphocytes: potential as a biological dosimeter. Health Physics 71(5): 687-693

3. Smith BP, Cregan SP, Mitchel REJ (1996) Apoptosis as measured by "ghost cell" frequency using the comet assay. Radiation Research, submitted.

Halo-Comet Assay

Juong Gile Rhee, Jie Liu, and Mohan Suntharalingam
Department of Radiation Oncology
University of Maryland School of Medicine
Baltimore, MD

Abstract

A simple procedure known as the "halo-comet" assay offers an accurate determination of changes in DNA organization (supercoiling) in individual cells; and the results are known to be equivalent to cell

survival. When x-rays were used, this assay was sensitive in detecting 0.5 Gy-induced changes of DNA organization prior to the damage repair, and 2.0 Gy-induced changes after the damage repair. This assay was also useful for protracted exposures to x-rays. When the image processing is automated, this assay could be a potential candidate for a field-capable means of dose estimation.

Introduction

The "halo-comet" assay is an extensively modified modern version of the fluorescence "halo" assay. The "halo" assay was originally described by Vinograd *et al.* [1] and refined by Roti-Roti *et al.* [2]. This assay quantifies the alterations of DNA organization (supercoiling) in individual cells; the results are known to be equivalent to cell survival [3]. Unfortunately, this assay has a limitation in its sensitivity. For example, this assay can detect changes in DNA organization at radiation doses on the order of 2 Gy prior to the damage repair [2]. However, when the damage is repaired, the assay becomes insensitive below 10 Gy [2, 4]. In order to increase the sensitivity, our laboratory has been involved in the modification of the "halo" assay, and has established the "halo-comet" assay, which can detect small amounts of damage in DNA organization even after the process of damage repair.

Materials and Methods

Two different cell lines were used. HL-60 human lymphoma cells were maintained in RPMI 1640 medium supplemented with 10% fetal bovine serum (GIBCO). MCF-7 human mammary carcinoma cells were maintained in IMEM medium supplemented with 10% fetal bovine serum, 10% HEPES, and zinc (GIBCO). Both cell lines were exponentially grown at the time of the experiments. A Seifert x-ray unit (Rich. Seifert & Co.) operated at 250 kVp, 15 mA with 0.5 mm copper plus 1.0 mm aluminum filtration was used to deliver radiation to the cells at a dose rate of approximately 2 Gy/min.

In order to produce the "halo-comet" structure, MCF-7 cells were dispersed into single cells with a trypsin solution. These dispersed MCF-7 cells, or HL-60 cells in suspension, were resuspended in a concentration of 10^5/ml in ice-cold PBS, and mixed with the same volume of a 2% agarose solution (Sigma, type I) that was dissolved in PBS and warmed at 60°C. The mixture was quickly spread onto a slide glass, allowed to form into a gel (less than a minute at room temperature), and stored in ice-cold PBS. Then the cells in the gel were exposed to a dye-lysis solution: a mixture of 2 mM Tris, 0.5% Triton X-100, 2 M NaCl and 10 mM EDTA (TTNE) with twice the desired propidium iodide (PI) concentration. Cell lysis was carried out in the dark at room temperature, and the lysis time was 15–30 min. Then the gel, after cell lysis, was washed in distilled water for 1h and subjected to electrophoresis in a TAE buffer (40 mM Tris, 20 mM acetic acid, and 5 mM EDTA). The time of electrophoretic separation was 20–30 min (3V/cm, 17 mA).

To visualize the "halo-comet" structure, the PI-stained DNA was excited at 545 nm; and the emission at 580 nm was observed with the aid of a 590 nm barrier filter under a reflected fluorescence microscope (Olympus, BH-2). The intensity of fluorescence light was enhanced using the Dark Invader Night Vision System (Meyers & Co. Inc.). The image was stored on video or digitized and processed with the use of an image processing software, Accuware (Automatic Visual Inspection).

Results and Discussion

In the modification of the existing "halo" assay, we first tried to produce the "halo" structure in an agarose gel, as opposed to producing it in a buffer solution, as described by Roti-Roti et al. [2]. This attempt was successful. We were able to observe the "halo" structure in an agarose gel (fig. 2, upper image). Since the structure was formed in an agarose gel, we tried applying an electric current to the gel, hoping that the DNA loops would be pulled from the "halo" structure. Following numerous attempts using different milliamperes and run times, the DNA loops were finally pulled toward the cathode.

The DNA loops were stretched and formed a tail (fig. 2, middle image). We prefer calling this tailed structure a "halo-comet" to distinguish it from the common names previously described as "halo" by Roti-Roti et al. [2], and "comet" by Olive et al. [5]. This "halo-comet" structure was indeed different from the alkaline "comet" structure (fig. 2, lower image), which was produced according to Olive et al. [5]. In the alkaline "comet" structure, there was a discontinuous distribution of fluorescence intensity from head to tail (fig. 2, lower image), suggesting that fragmented DNA strands were separated (tail) and removed from the nuclear matrix (head). In this assay, DNA damage (single strand breaks) is quantified in terms of a "tail-moment," a product of the amount of DNA removed from the head and the distance of migration [5]. In contrast to the "comet" image, the "halo-comet" image showed a continuous fluorescence distribution (fig. 2, middle image), implying that DNA loops were still attached to the nuclear matrix and were stretched from the matrix by electric charges. Since no head and tail was distinguishable, it was impractical to quantify the "halo-comet" image in terms of a "tail-moment." Therefore, the longest axis (image length) or pixel numbers (image area) occupied by the "halo-comet" image were determined to quantify the damage of DNA organization.

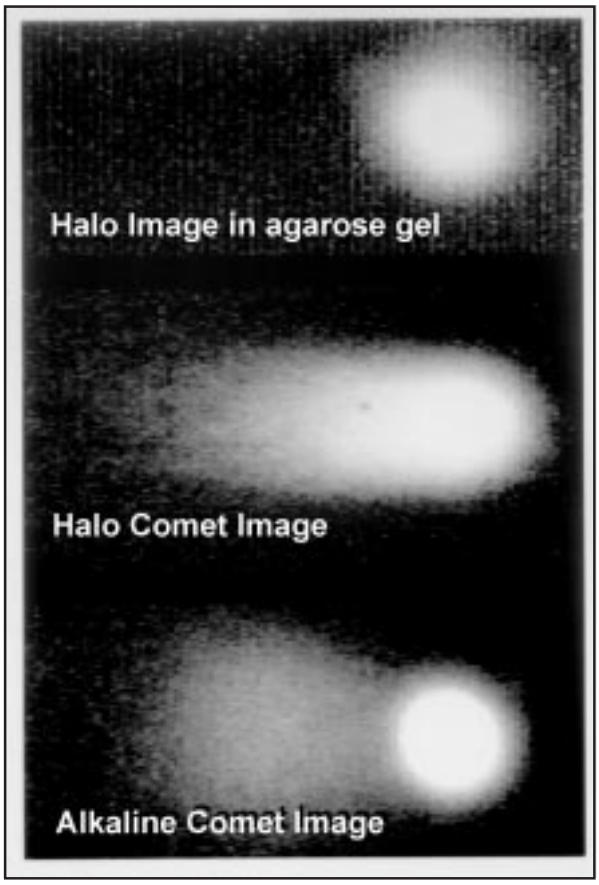

Fig. 2. Comparison of different images of HL-60 cells. The "halo" image was formed in an agarose gel (top). The "halo" structure was stretched by electrophoresis to form a "halo-comet" image (middle). An alkaline "comet" image (bottom) was quite different from the "halo-comet" image (middle).

To optimize the assay, the concentration of PI was varied (0–50 μg/ml). When control (0 Gy) cells were used, the "halo-comet" structure became larger with increasing PI concentration. The largest structure was maintained when the PI was higher than 10 μg/ml. For irradiated (20 Gy) cells, the largest structure was observed when the PI was higher than 30 μg/ml. Since a maximal difference between the control and the irradiated cells was observed at 30 μg/ml, this PI concentration was chosen as a standard. When HL-60 and MCF-7 cells were irradiated (0–20 Gy) and subjected to the "halo-comet" assay, the amount of DNA pulled from nucleoids (nuclei remaining after removal of proteins) increased linearly with increasing radiation doses up to 6 Gy (data are not shown). The sensitivity of the "halo-comet" assay was found to be far greater than that of the existing "halo" assay. For instance, the changes in DNA organization following doses as low as 0.5 Gy prior to the damage repair were detected by the "halo-comet" assay, which is a significant advancement over the existing "halo" assay. For the "halo-comet" assay, differences between the 0 Gy versus 0.5 Gy-induced damage was statistically significant ($p < 0.05$, Student-t test), either when analyzed for image area by 50 samples or when analyzed for image length by 25 samples (data are not shown).

Since the "halo-comet" assay can detect 0.5 Gy-induced alterations of DNA organization, we attempted the detection of residual alterations of DNA organization remaining after the repair processes. MCF-7 cells were exposed to 0, 2, and 4 Gy of x-rays and were incubated at 37°C for 30 min. These cells were then subjected to a gel formation and to the "halo-comet" assay. The resultant "halo-

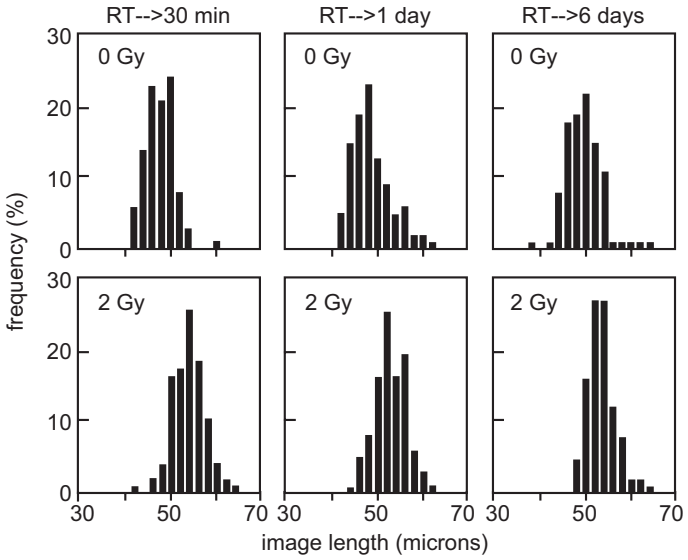

Fig. 3. Residual damage remained after the repair processes. MCF-7 cells were exposed to x-rays and incubated for 30 min. These cells were then subjected to the "halo-comet" assay by employing two image parameters. For each group, 100 images were analyzed.

comet" images were analyzed in terms of both image length and area; the results are shown in fig. 3. For both image length and area, a distinction between the control and 4 Gy-irradiated cells appeared to be clear; so only the paired data sets for 0 versus 2 Gy data were subjected to the Student-t test. As shown in table 1, the difference between 0 and 2 Gy data was highly significant ($p < 0.0004$) with samples as small as 25 for both endpoints. This sensitivity is superior to the sensitivity of the "halo" assay, which can only detect a difference between 0 and 10 Gy of DNA damage after the repair processes [4]. When HL-60 cells were used, the "halo-comet" assay was able to detect 2 Gy-induced alterations of DNA organization even 1 or 6 days after the irradiation, as shown in fig. 4, where the endpoint of the assay was image length.

Table 1. Student t-test (p values) for the changes in DNA organization induced by 0 versus 2 Gy of X-rays. "Halo-comet" assay was performed after completion of the repair processes.

Sample size	Image area	Image length
25	0.000024	1.2×10^{-12}
50	9.9×10^{-10}	$< 10^{-16}$
100	0.000333	$< 10^{-16}$

Since residual alterations of DNA organization (2 Gy) remained after repair processes were detectable (figs. 3 and 4), we attempted to study the effect of a

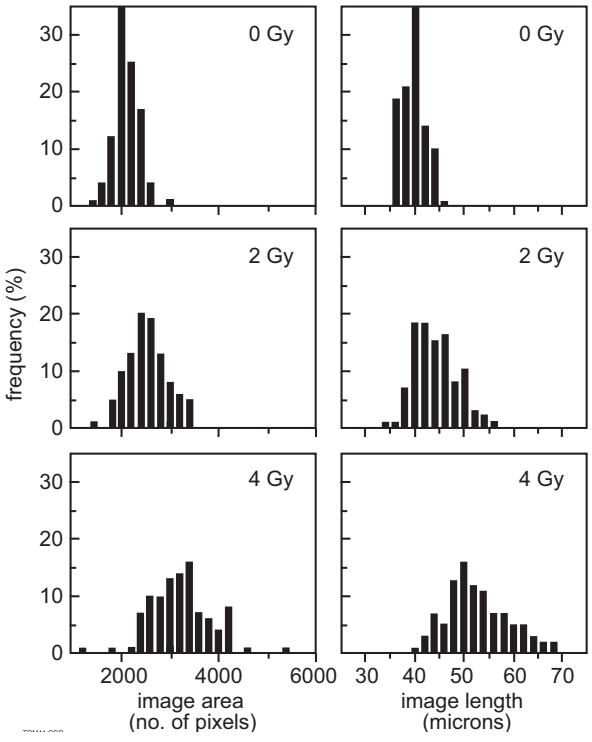

Fig. 4. Residual damage remained even after 6 days of recovery. HL-60 cells were exposed to x-rays and incubated for up to 6 days before the "halo-comet" assay. The image was analyzed in terms of image length; 100 images were analyzed for each group.

protracted exposure to x-rays. MCF-7 cells were exposed to daily 2 Gy doses for 3 days (Monday, Tuesday, and Wednesday). The changes in DNA organization were determined on the following Monday. As shown in fig. 5, the amount of damage increased with increasing number of exposures or increasing total doses, when determined by image area. Although the assay was carried out 5 days after the completion of daily exposures, dose-dependent alterations of DNA organization were clearly observed.

As demonstrated in the present report, the "halo-comet" assay has great potential as a field-capable means for dose estimation. This assay is based on a non-radioactive procedure, and is sensitive to 2 Gy-induced genotoxicity. The result of this assay is known to be equivalent to cell survival [3]. This assay can handle a large number of samples simultaneously. For example, processing 100 samples may not be difficult for trained personnel, since four different samples can be loaded onto a slide glass; and 25 slides may be loaded for electrophoresis at the same time. Another advantage is the speed of the assay. The "halo-comet" images can be produced in less than 2 h for every set of sample loading. For dose estimation, these produced images need to be analyzed by using an image processor. When 100 images for each sample are to be analyzed, for example, a total of 10,000 images for 100 different samples must be analyzed. Therefore, automating the image processing is essential to shorten the time for dose estimations of a large volume of samples; the overall time required for dose estimations might depend on the success of the automation. Many variables that will affect the "halo-comet" assay have not been determined. Further studies are absolutely necessary to optimize the assay for a field-means of dose estimation.

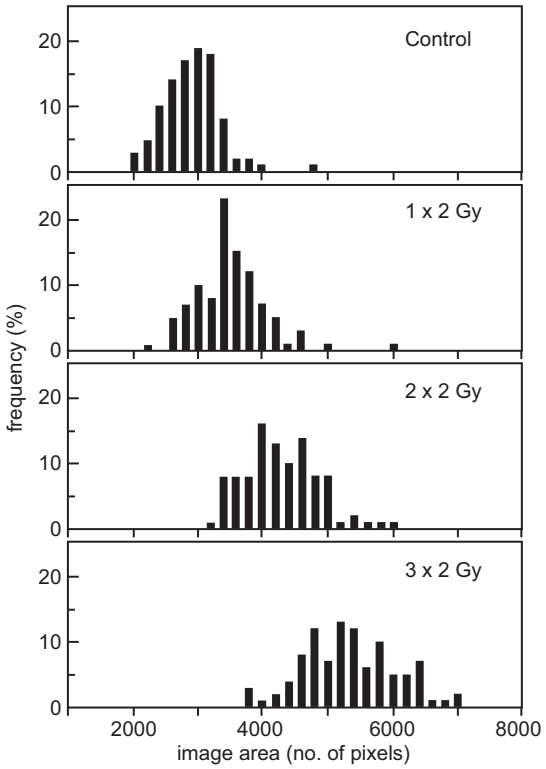

Fig. 5. Persistent residual damage remained after protracted exposures. MCF-7 cells were exposed to control, 1 x 2 Gy, 2 x 2 Gy, and 3 x 2 Gy of x-rays as described in test above. The "halo-comet" assay was carried out 5–7 days after irradiation. Residual damage remained after repair and was dose-dependent.

References

1. Vinograd J, Lebowitz J, Radloff R, Watson R, Laipis P (1965) The twisted circular form of polyoma viral DNA. Proc. Natl. Acad. Sci. USA 53:1104-1111

2. Roti Roti JL, Wright WD (1987) Visualization of DNA loops in nucleoids from Hela cells: assays for DNA damage and repair. Cytometry 8:461-467

3. Malyapa RS, Wright WD, Roti Roti JL (1995) Possible role(s) of nuclear matrix and DNA loop organization in fixation or repair of DNA double-strand breaks. In: Fuciarellli AF and Zimbrick JD (eds) Radiation Damage in DNA, Battelle Press, pp 409-426

4. Jaberaboansari A, Nelson GB, Roti Roti JL, Wheeler KT (1988) Postirradiation alterations of neutronal chromatin structure. Radiat. Res. 114:94-104

5. Olive PL, Banath JP, Durand RE (1990) Heterogeneity in radiation-induced DNA damage and repair in tumor and normal cells measured using the "comet" assay. Radiat. Res. 122:86-94

Radiation Damage in the Hematopoietic System

Lionel G. Filion[1], *Kelley A. Chambers*[1], *and William M. Ross*[2]
[1]Department of Microbiology and Immunology
University of Ottawa
[2]Department of Physiology, University of Ottawa
[2]Defense Research Establishment Ottawa
Ontario, Canada

Abstract

After exposure to ionizing radiation, even at sublethal doses, the cellularity and functional capacity of the immune system is compromised. This leads to increased susceptibility to disease and infection. The degree of impairment needs to be assessed. We have found that flow cytometry (FCA) is potentially one of the fastest, most accurate methods to achieve this. We have examined alterations in all of the major splenic and peripheral blood mononuclear cell populations in C57BL/6 mice following whole-body irradiation (0–700 cGy) to determine which cell populations may play a role in active immune suppression and/or hematopoietic recovery. A flow cytometric protocol has been established for the characterization and differentiation of the major mononuclear cell populations in the mouse spleen and whole-blood: T lymphocytes ($CD4^+$ and $CD8^+$ cells), B lymphocytes ($CD45^+$), natural killer (NK) cells, and monocytes/macrophages. Ionizing radiation caused decreased cellularity in both the splenic and whole-blood cells. In addition, the induction of apoptosis in the blood cells was assessed by the measurement of phosphotidylserine with the use of Annexin V. FCA revealed alterations in the relative composition of the constituent cell populations following irradiation, reflecting differential radiosensitivity, with selective enrichment of NK cells and $CD4^+$ T lymphocytes. Enrichment developed and persisted during the 7-day post-irradiation period. Some mononuclear cells became activated in a dose and time-dependent fashion following whole-body irradiation (WBI), as indicated by expression of CD71, the transferrin receptor. These cells were $CD34^+$ and $Thy1.2^+$ but were $CD4^-$ and $CD8^-$, as well as $CD45R^-$. The observed increase in NK cells corresponds to a previously reported increase in natural suppressor (NS) cells following total-lymphoid irradiation (TLI). The balance of recovery-inhibiting NK cells and recovery-enhancing $CD4^+$ T lymphocytes following irradiation may reflect or influence the degree of hematopoietic recovery, and may provide an indication of the extent of damage (biological dosimetry).

Introduction

Exposure to ionizing radiation can render the immune system incompetent due to systemic damage to the hematopoietic system. The ultimate survival of an animal following irradiation depends largely on the recovery of blood-cell formation. The hematopoietic capacity of the bone marrow, the organized lymphoid tissues, and individual small recirculating lymphocytes are all exquisitely radiosensitive. Since this system provides for renewal of mature circulating blood cells, those cells killed by irradiation or used up performing their functions will not be replaced until stem-cell recovery occurs. The recovery requires a sufficient number of surviving endogenous stem cells to proliferate, restore the stem cell pool, and provide specific progenitor cells which will differentiate into functionally mature cells. This process is regulated by a variety of cytokines which are produced by cells that constitute the hematopoietic microenvironment, including stromal elements and monocytoid accessory cells from peripheral blood [1-3]. The recovery of the hematopoietic system in mice given bone marrow transplants has been demonstrated to be enhanced by a distinct $Thy\text{-}1^+$ subpopulation resistant to radiation and cyclophosphamide [4]. The fact that such cells appeared to be relatively radioresistant and that a small population of radioresistant $Thy\text{-}1^+$ lymphocytes were found to survive *in vivo* in heavily irradiated animals [5] suggests that these cells may play a role in facilitating hematopoietic recovery. While the role of the $CD4^+$ T cell subset in hematoregulation has recently come under investigation [6-8], the relative radiosensitivities of the CD4 and CD8 subpopulations of T lymphocytes compared to other mononuclear cell populations have not been well characterized *in vivo* after irradiation.

This study was undertaken, using a murine model, to examine alterations in the major whole blood and

splenic mononuclear cell populations and their state of activation following whole-body irradiation (WBI). We employed flow cytometric analysis (FCA) using monoclonal antibodies to characterize and differentiate the various cell types by their specific and unique cell surface markers (CD), including CD71, the transferrin receptor [9, 10]. The induction of apoptosis was also determined by the measurement of Annexin V binding. The working hypothesis was that the relative concentration of certain cells is altered by irradiation, and this leads to the occurrence of immune system dysfunction or failure. It is our aim to identify particular alterations in relative cell number that might correlate with the dose received, the extent of resultant injury, and the immune-competent status of the animal.

Materials and Methods

C57BL/6 mice used in this study were female, weighed 18–20 g, and were obtained from Charles River (Montreal, Canada). The mice were housed in cages of five in the animal-care facility at the University of Ottawa, and given Purina Mouse Chow pellets and acidified water (pH=2.7) *ad libitum*.

Irradiation of mice was conducted in a ^{137}Cs GammaCell-40 shielded-drawer radiation source (Nordion, Kanata, ON, Canada) at a dose rate of 110 cGy/minute.

Whole blood samples were drawn by bleeding mice from the retro-orbital sinus, and prepared for flow cytometric analysis (FCA). Blood or spleen cells were stained with various combinations of fluorescently-labeled monoclonal antibodies or Annexin V -FITC and propidium iodide as listed in table 2. Samples were taken on days 1, 4, and 7 after exposure to WBI (25 to 700 cGy). Staining of blood and spleen samples was followed by lysis of contaminating erythrocytes and subsequent analysis by flow cytometry on a Coulter Epics XL flow cytometer (Coulter Electronics, Hialeah, FL).

Cell number was assessed by analysis on a Coulter-Zm Counter (Coulter Electronics). 20 µl of whole blood were diluted in 10 ml of Isoton II diluent (Coulter Electronics), treated with three drops of Zap-o-globin II (Coulter Electronics) for erythrocyte lysis.

Table 2. Panel of reagents employed for flow cytometric analysis.

Tube	Reagent	Cell marker
1	None	
2	Isotype controls	
3	Thy 1.2-PE CD4-FITC	T cells and CD4 T cell subset
4	Thy 1.2-PE CD8-FITC	T cells and CD8 T cell subset
5	CD45R-FITC	B cell
6	NK 1.1-PE	NK cell
7	MAC-FITC	Macrophage
8	Annexin V-FITC Propidium iodide	Apoptosis marker

Results

Blood drawn from mice on days 1, 4, or 7 after exposure to 100, 400, or 700 cGy WBI was stained according to the combinations of mAb in table 2, in order to identify numbers and percentages of individual peripheral blood mononuclear cell populations by flow cytometry. Figure 6 (a and b)

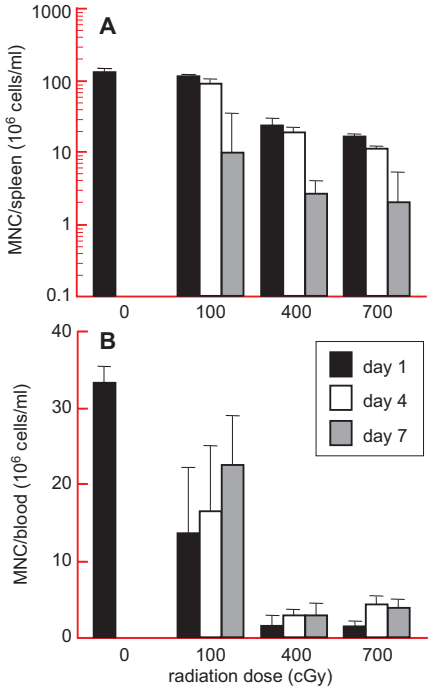

Fig. 6. Effect of radiation on the cellularity of spleen and blood.

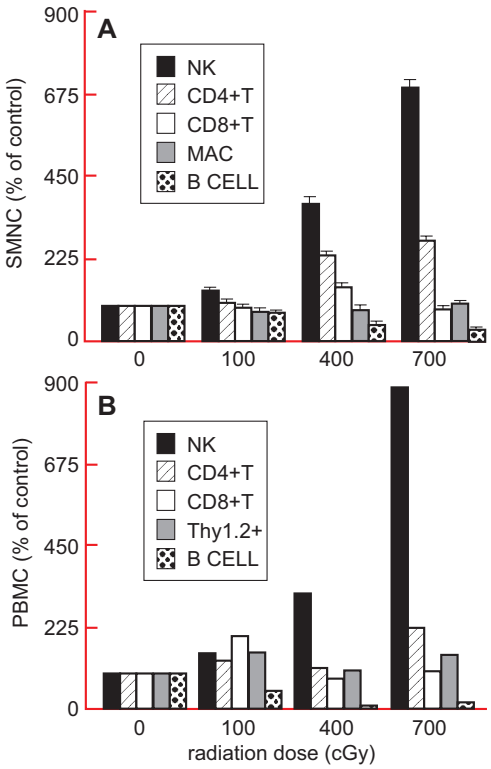

Fig. 7. Relative sensitivities of subpopulations of SMNC and PBMC to radiation.

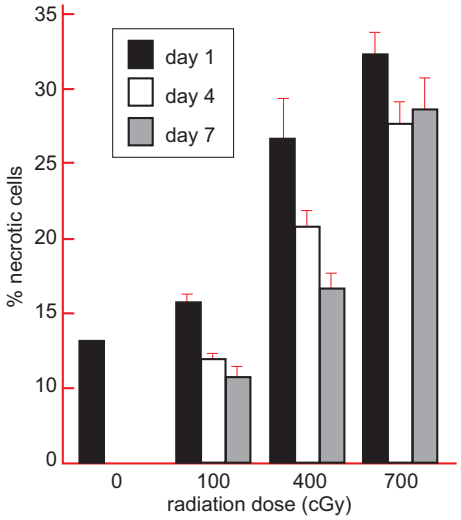

Fig. 9. Kinetics of appearance of necrotic cells in the periphery.

demonstrates a dose-dependent decline in the total leukocyte count (splenic or whole blood) with increasing radiation dose.

Figures 7a and 7b show the alterations in the relative proportions of MNC populations on day 4 after radiation exposure, for the peripheral blood (PBMC) and spleen (SMNC), respectively. Clearly, in both compartments, B lymphocytes exhibit dramatic radiosensitivity; while NK and $CD4^+$ cells demonstrate marked radioresistance. Other MNC types appear to show no statistically significant changes in their relative proportions after radiation exposure.

In figure 8, a population of cells morphologically distinct from normal blood MNC, as determined by flow cytometry, appears after radiation exposure. These cells are more granular than typical lymphocytes or monocytes, a feature characteristic of apoptotic cells. The prevalence of this population of cells is dose-dependent and declines with time, as shown in figure 9.

Figure 10 (a and b) demonstrates the radiation and time dependent Annexin-V response of the lymphocyte population. As early as 1 hour postirradiation, AnnexinV binding was observed with only 25 cGy. The more granular population observed in figure 9 was 100% for Annexin V and propidium iodide.

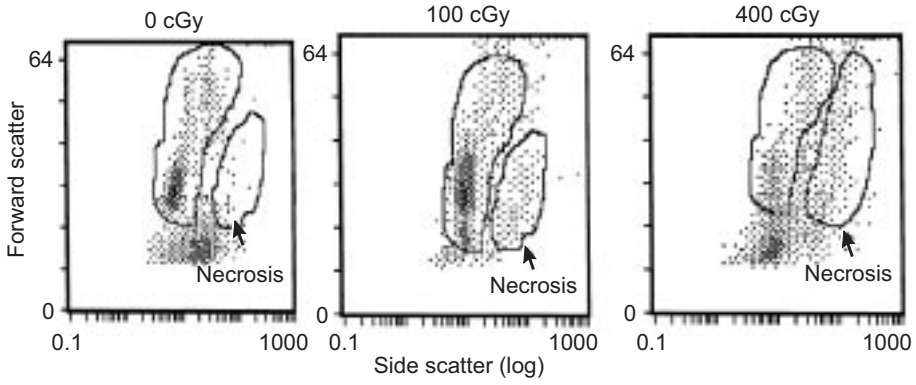

Fig. 8. Changes in size (FS) and granularity (SS) with radiation dose.

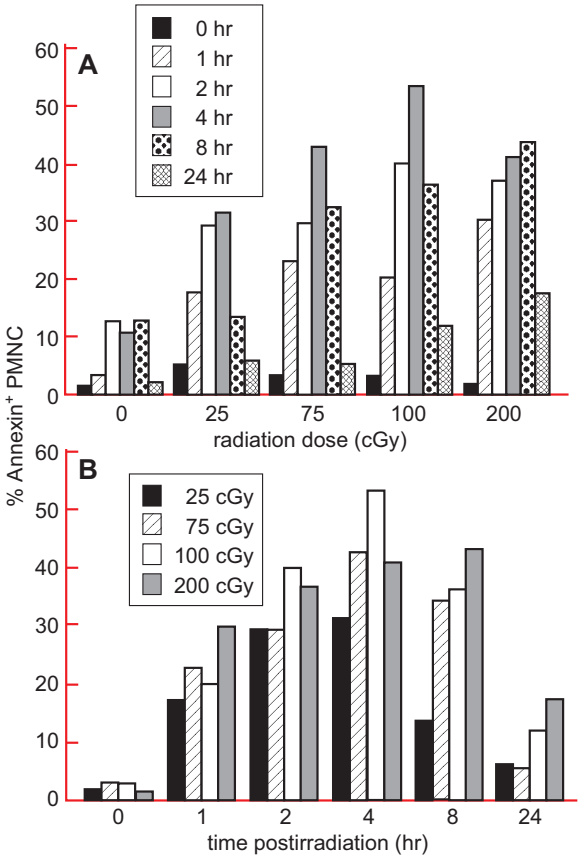

Fig. 10. Annexin response of PBMC after irradiation.

This indicates that these cells were in the apoptotic or necrotic phase.

Tables 3 and 4 reflect the presence of CD71, the transferrin receptor; this marker can be found on cells that are differentiating. CD71 is found on a small proportion of splenic or peripheral blood leucocytes (3–4%) from unirradiated mice. All doses of radiation (100–700 cGy) failed to increase the percentage of positive cells on day 1 post-WBI. But higher levels of CD71-expressing cells were

Table 3. Percentage of CD71+ cells after whole body radiation.

Day	Control	100 cGy	400 cGy
1	1	3	3
4	3	9	3
7	3	11	2

Table 4. CD71 expression on cell subtypes.

Marker	% $CD71^+$
CD34	13
Thy1.2	13
CD4	0
CD8	0
CD45R	0
Macrophage	0
NK1.1	0

observed at different times and after different exposure doses (table 3). The population expressing the CD71 molecule was identified as $CD34^+$ or $Thy1.2^+$. Other markers were also tried but the CD71 cells were negative for these: CD4, CD8, B-cell marker CD45R/B220, macrophage marker $F4/80^+$, and NK1.1 (table 4).

Discussion

Suppressor-cell activation and severe damage to the bone marrow stem-cell population are two adverse effects resulting from exposure to ionizing radiation [11-13] which increases susceptibility to opportunistic infections. In the present study we have examined the relative radiosensitivity of SMNC and PBMC populations following whole-body irradiation. Such alterations may be indicative of a role for a particular subpopulation in active immune suppression or in hematopoietic recovery, and may be useful as an early biological marker for severity of damage to the critical immune system, and thus as an effective prognostic indicator for triage.

Whole-body irradiation of mice produced an exponential decline in cell survival of splenic cells and peripheral blood leukocytes in whole blood (fig. 6) as has been previously demonstrated both *in vitro* and *in vivo* [14]. The relative proportions of the mononuclear cell subsets in both organs dramatically

changed (figs. 7a and 7b) and were similarly affected. We examined changes in the major mononuclear cell populations in both organs including B lymphocytes, the $CD4^+$ and $CD8^+$ subsets of T lymphocytes, monocyte/macrophages and natural killer cells. Although all cell populations declined, they did so at different rates. In increasing order of radiosensitivity were: NK cells (D_0= 4.8Gy $\pm$ 0.8Gy), $CD4^+$ T cells (D_0= 3.1 $\pm$ 0.6), $CD8^+$ T cells (D_0= 2.2 $\pm$ 0.4), monocytes/macrophages (D_0= 1.7 $\pm$ 0.1), and B cells (D_0= 1.5 $\pm$ 0.1). The natural killer cells in this study were the most strikingly radioresistant cell population of the PBMC or SMNC. In control mice, NK cells made up only a small fraction on the total population (3%); whereas 7 days after 400 cGy irradiation, NK cells comprised almost one-quarter of the total PBMC or SMNC (results not shown).

The relatively high sublethal doses of radiation used in these studies induced hematopoietic depletion that was followed by vigorous recovery initiated from endogenous stem and progenitor cells that survived the irradiation [14]. *In vitro* studies have demonstrated that different lymphoid subsets have opposing effects on hematopoietic cell growth [15,16]. The hematopoietic recovery of an irradiated animal may then be influenced by the proportions of surviving recovery-enhancing and recovery-inhibiting cell types. T lymphocytes have been found to consist of two distinct subpopulations: a radioresistant population which can enhance hematopoietic recovery, and a radiosensitive population which can suppress it [4, 17]. However, the relationship of such subpopulations to the immunoregulatory $CD4^+$ helper and $CD8^+$ suppressor T lymphocytes has not been determined; but it has been recently reported that $CD4^+$ cells are stimulators of normal hematopoiesis and recovery following whole-body irradiation [7, 18]. The results reported here are in agreement with Williams et al. [7] in that the murine spleen contains a population of radioresistant $CD4^+$ T cells. As a result of the radioresistance of these cells, the spleens of irradiated mice became proportionately "enriched" with $CD4^+$ T cells. By 7 days post-700 cGy WBI, $CD4^+$ lymphocytes made up almost 50% of all SMNC, as compared to only 15% in control mice. The differing radiosensitivities of $CD4^+$ and $CD8^+$ T lymphocytes observed in the spleen are comparable to the radiosensitivities of the different types of T cells that exert helper and suppressor effects on hematopoietic recovery [17].

The type of cells expressing CD71 was demonstrated to be $CD34^+$ and $Thy1.2^+$; but they were not positive for CD4, CD8, CD45R/B220, or NK1.1. This suggests that CD71 is expressed on early progenitor cells and may be an indicator for early hematopoietic activity or possibly dedifferentiation (reactivation of dormant gene for CD71 expression, normally only functional during cell differentiation and development). CD34 and Thy1.2 account for 56% of the CD71 positive cells. The remaining cells may be other lineage specific cells. The absence of T cell subset markers (CD4 or CD8) also suggests that the $CD71^+$ cells are immature T cells that appear in the periphery after radiation or are somehow activated (19).

Our findings to date support the hypothesis that the relative decline in certain immune subpopulations is indicative of damage to and impairment of the immune system. For a biological "dosimeter," changes in proportion of cell types detected by flow cytometry represent a rapid way of assessing damage after radiation exposure and may also serve to assess the effectiveness of radioprotective agents in animal models or tissue culture.

Acknowledgments

The financial assistance and support of the Defence Research Establishment Ottawa, Department of National Defence, Ottawa, Canada, is gratefully acknowledged. Kelley Chambers is a recipient of an Ontario Graduate Student Scholarship.

References

1. Dexter TM, Allen TC, Lajtha LG (1977) Conditions controlling the proliferation of hematopoietic stem cells *in vitro*. J Cell Physiol 91: 335-344

2. Torok-Storb B (1988) Cellular interactions. Blood 72:373-381

3. Itoh K, Tezuka H, Sakoda H, Konno M, Nagato K, Uchiyama T, Uchino H, Mori KJ (1989) Reproducible establishment of hematopoietic supportive stromal cell lines from murine bone marrow stroma. Exp Hematol 17:145-153

4. Sharkis SJ, Spivak JL, Ahmed A, Misti J, Stuart RK, Wiktor-Jedrzejczak W, Sell KW, Sensenbrenner L (1980) Regulation of hematopoiesis: helper and suppressor influences of the thymus. Blood 55:524-527

5. Anderson RE (1976) Ionizing radiation and the immune response. Adv Immunol 24:215-235

6. Kanz L, Lohr GW, Fauser AA (1986) Lymphokine(s) from isolated T lymphocyte subpopulations support multilineage hematopoietic colony and megakaryocytic colony formation. Blood 68:991-995

7. Williams JL, Patchen JL, Darden JH, Jackson WE (1994) Effects of radiation on survival and recovery of T-lymphocyte subsets in C3H/HeN mice. Exp Hematol 22:510-516

8. Bonomo AC, el-Cheikh MC, Borojevic R, Cavalcante LA, DosReis GA (1990) Comparative analysis of splenic cell proliferation induced by interleukin-3 and by syngeneic accessory cells (syngeneic mixed leukocyte reaction): evidence that autoreactive T cell functioning instructs hematopoietic phenomena. Cell Immunol 125: 210-224

9. Taetle R, Honeysett JM (1988) IFN-gamma modulates human monocyte/macrophage transferrin receptor expression. Blood 71:1590-1595

10. Schlossman SF, Boumsell L, Gilks W, Harlan JM, Kishimoto T, Morimoto C, Ritz J, Shaw S, Silverstein RL, Springer TA (1994) Leucocyte Typing V: white cell differentation antigens. Proceedings of the Fifth International Workshop and Conference; International Conference on Human Leucocyte Differentiation Antigens. Oxford : Oxford University Press

11. Oseroff A, Okada S, Strober S (1984) Natural suppressor (NS) cells found in the spleen of neonatal mice and adult mice given total lymphoid irradiation (TLI) express the null surface phenotype. J Immunol 132:101-110

12. Strober S, Slavin S, Gottlieb M, Zan-Bar I, King DP, Hoppe RT, Fuks Z, Grumet FC, Kaplan HS (1979) Allograft tolerance after total lymphoid irradiation (TLI). Immunol Rev 46:87-112

13. Waer M, Ang KK, Van der Schueren E, Vandeputte M (1984) Allogeneic bone marrow transplantation in mice after total lymphoid irradiation: influence of breeding conditions and strain of recipient. J Immunol 132:991-996

14. Coggle JE (1993) Biological effects of radiation. London: Wykeham Publications

15. Pantel K, Nakeff A (1989) Lymphoid cell regulation of hematopoiesis. Int J Cell Cloning 7:2-12

16. Pantel K, Nakeff A (1993) The role of lymphoid cells in hematopoietic regulation. Exp Hematol 21:738-742

17. Sharkis SJ, Colvin MO, Sensenbrenner L (1981) Effect of radiation and 4-hydroperoxycyclophosphamide on thymic regulators of erythropoietic growth. Stem Cells 1:269-275

18. Pantel K, Nakeff A (1990) Differential effect of $L3T4^{+}$ cells on recovery from total-body irradiation. Exp Hematol 18:863-872

19. Harrington NP, Chambers KA, Ross WA, Filion LG (1997) Radiation damage and immune suppression on splenic mononuclear cell populations. Clin Exp Immunol 107:417-424

Automated Cytogenetic Assays in a Field Environment: Consideration of the Halo-Comet Assay

Harry L. Loats[1], *Donald G. Lloyd*[1], *Tracy Roberge*[1], *and William F. Blakely*[2]
[1]Loats Associates, Inc., P.O. Box 528
Westminster, MD
[2]Armed Forces Radiobiology Research Institute
Bethesda, MD

Abstract

Cytogenetic-based bioindicator assays can provide diagnostically important information in forward-field military environments. In addition to assessing the effective equivalent biological dose, these assays provide estimates of the fraction of the body spared from radiation exposure. Based on its minimal pre-scoring preparation requirements, the halo-comet assay was identified as having potential for inclusion in a multi-assay system that can be used in the forward field. This paper's objective is to discuss the potential patient throughput of an automated halo-comet scoring system optimized for radiation biodosimetry.

Radiation Biodosimetry Requirements in the Forward Field

The following considerations were established to define candidate high-throughput automated cytogenetic assay systems relevant to field-level radiation biodosimetry. Since sample preparation requirements generally limit their echelon I medical facility utility, cytogenetic-type assays are generally focused on echelon II and III facilities. These assays in military scenarios require significant per patient sampling and also require high patient throughput for radiation biodosimetry triage. For processing in the triage mode, 20–50 cells per patient are required; in the dose assessment mode, 50–300 cells per patient are required. Typical patient throughput requirements range from 50–500 patients per day. In addition to minimized weight and footprint requirements, the field system must be simple to operate by non-specialist personnel.

Table 5 lists the existing cytogenetic assays which are potential candidates for inclusion in a radiation biodosimetry multi-assay platform that can be fielded in echelon II and III medical facilities. Of the assays listed, the halo-comet assay exhibits both minimal pre-scoring cell processing properties and has the signal persistence sufficient to accommodate field use. The halo-comet assay does not require post-sampling incubation and is characterized by short processing time requirements. From a post-preparation scoring perspective, the comet and apoptosis assays can be considered as a subset of the halo-comet assay.

Halo-Comet Scoring

The halo-comet assay is based on nuclear suspensions in contrast to the normal comet assay that uses whole-cell suspensions. Nucleoid samples are isolated after an interval sufficient to complete early strand-break repair. At this time point, the halo-comet

Table 5. Potential biodosimetry cytogenetic assays.

Assay	Sample type	Post-sampling incubation (37°)	Processing	Persistence
Halo-comet	Blood	No	Short	Yes
Comet	Blood/tissue	No	Short	No
Apoptosis	Blood	No	Short	Yes
Dicentric	Lymphocyte	Yes (48 hr)	Long	Yes
PCC/Dicentric	Lymphocyte	Yes (30 min)	Short, complex	Yes

assay focuses on persistent DNA conformational effects, which can be used as a radiation biodosimetry assay system. The halo-comet assay has the potential to estimate partial-body exposure effects.

The halo-comet assay can also measure cell apoptosis, which can be considered a complementary or alternative biodosimetry measure. Most of the DNA in apoptotic comets moves from the comet's head into the tail. The apoptotic cell-tail moment is generally a factor of 15X to 30X greater than that exhibited by normal cells under standard assay conditions. The cytogenetic halo-comet assay allows detection of a higher fraction of apoptotic cells at an earlier time in comparison to flow cytometric methods.

The halo-comet scoring is the same as that performed for the normal comet assay. The principal halo-comet scoring measures include: 1) tail length which measures the distance of DNA migration from the nucleus, and 2) the tail moment which is the product of the tail length and the fraction of total DNA in the tail. The tail moment incorporates both size of migrating DNA (reflected in the comet tail length) and the number of fragments (represented by the intensity of DNA in the tail). Bivariate analysis using both DNA damage and DNA content is used to define subtle changes in response to various treatments in cells within the cell cycle.

Automated Halo-Comet Analysis System Design

The automated halo-comet cytogenetic system has been designed around existing hardware. The rapid automated cell-finding capability incorporated into the present design is based on the experience gained from developments and improvements of the automated metaphase finder, currently in service in the AFRRI Biodosimetry Laboratory (fig. 11). A cartridge-type slide container which can serve as a basis for slide preparation is

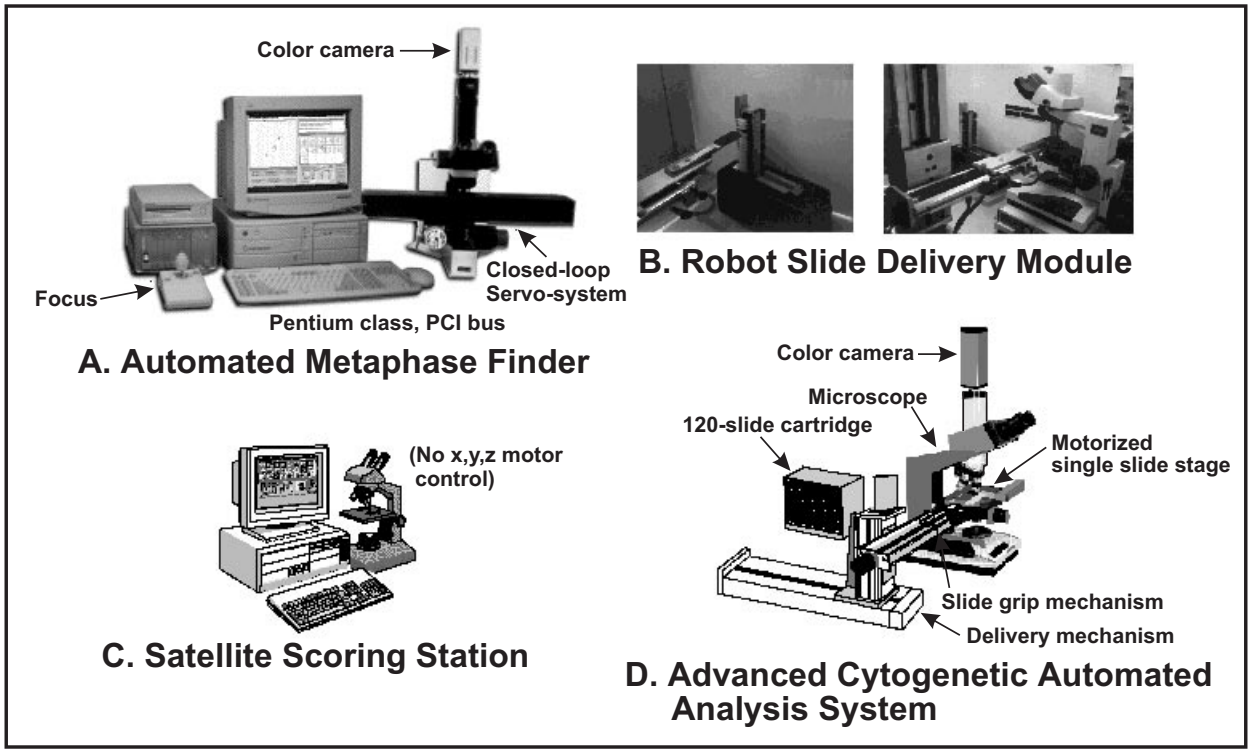

Fig. 11. Available hardware for cytogenetic assay automation. The automated halo-comet assay is based on modifications to the existing automated cytogenetic assay designed for Metaphase spread finding and analysis. The LAI Automated Metafind System (A) typifies the current state of cytogenetic assay automation. Important enabling extensions to this technology include an automated robotic slide delivery module (B) and stand-alone satellite scoring stations (C) that increase assay scoring throughput. An advanced system configured for use in the pharmaceutical industry is shown in panel (D). This system incorporates the large capacity robot slide delivery module required to accommodate high throughput requirements.

incorporated. Servo-controlled slide selection and delivery components are computer controlled. This capability is incorporated into the system that is intended for use in the field.

The LAI comet assay system employs a specially gated, cooled CCD camera that enhances the signal during image acquisition by integrating multiple acquisition frames. Comet images are automatically corrected for background and are analyzed as acquired. Non-target cells are automatically excluded from the analysis. An automated texture-based algorithm is used to define the discontinuous boundary of the comet tail.

Figure 12 illustrates the output of the LAI automated comet scoring system. Specific analysis parameters include: moment, moment arm, total-tail intensity, tail area, tail length, percent of tail DNA. Head and tail profiles are overlaid on each display. Group histograms of measured parameters are displayed and updated as the comets are acquired. Group statistics are available immediately upon completion of group acquisition. Histograms of group statistics are also continually displayed.

Multi-Channel Automated Halo-Comet Scoring System

The design guidelines adopted for the adaptation of the current automated comet assay system to accommodate military forward-fielding requirements are: 1) incorporation of minimized micro-optics, 2) incorporation of electronic zoom, 3) parallel cell search and analysis, and 4) the provision of multiple cell analysis channels. These criteria were

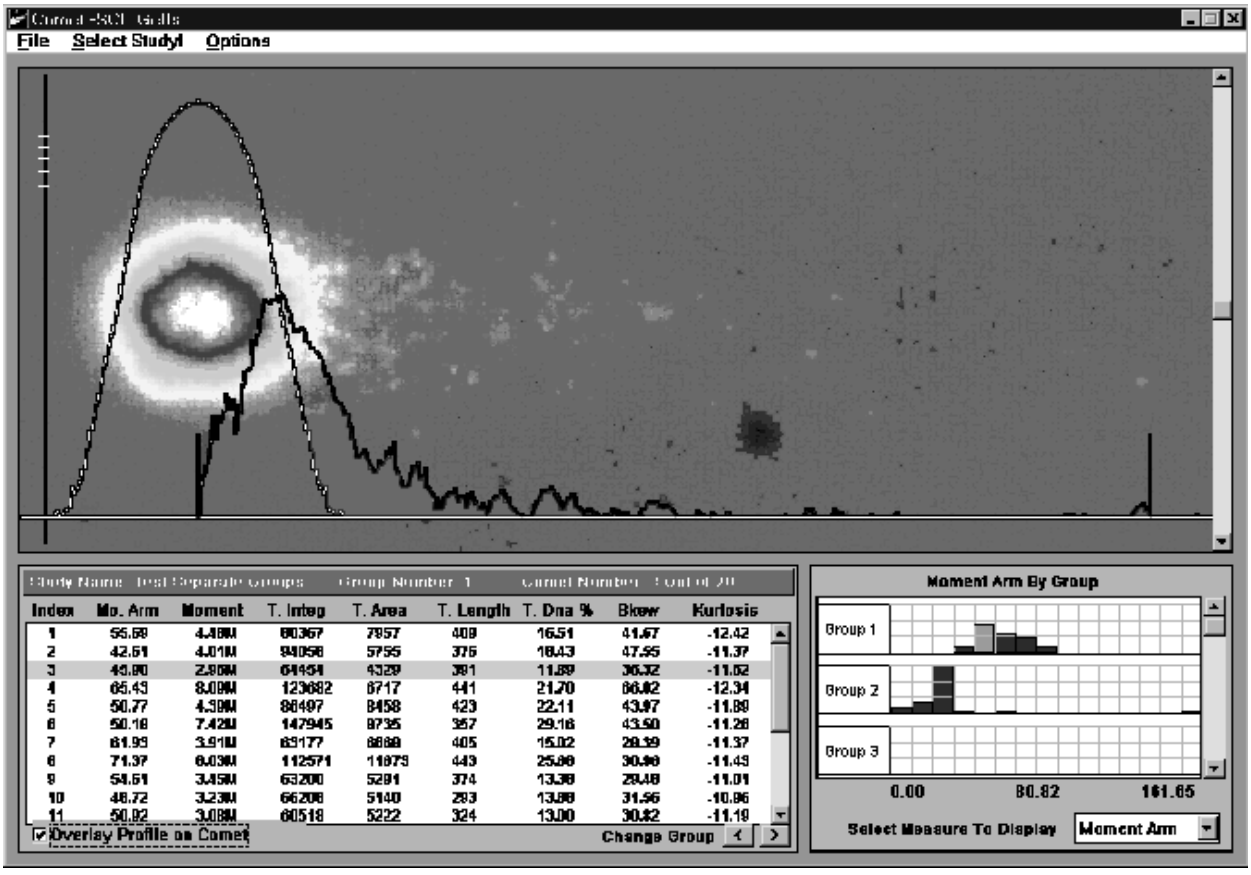

Fig. 12. Current comet assay system at LAI. Shown here is the computer display of the LAI Automated Comet Assay program displaying a typical cell which has been automatically acquired and analyzed. The program searches and locates individual cells and automatically separates the comet head and tail. Quantitative measures include tail area, tail length and tail moment. Group statistics are accumulated as required.

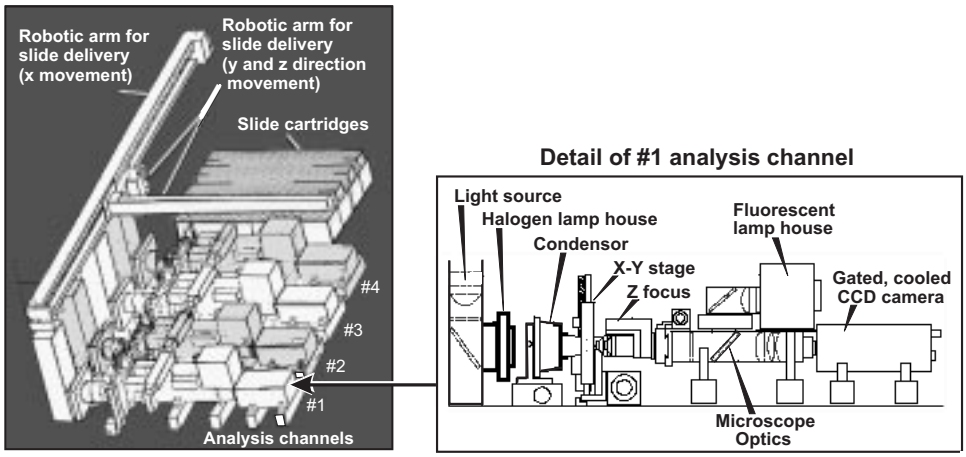

Fig. 13. Halo comet field automated analysis system. This figure illustrates the design of a parallel multi-channel system proposed for the halo-comet assay. Individual slides are presented to the optical analysis channel by the robot slide delivery module. The fluorescent cell images are acquired with a special gated, cooled CCD camera acquisition module that provides a 12-bit image capture capability that is necessary to span the dynamic range of the cell images.

incorporated into the design of the multi-channel automated halo-comet system (fig. 13).

The special features of this system include: 1) automated cell finding, 2) a new technique for image acquisition based on low-light level range extension to provide dynamic range extension, 3) a digital method to produce a composite image from a series of closely spaced images neighboring the plane of best focus, and 4) parallel cell finding and analysis.

Throughput Estimation for the Automated Halo-Comet Assay

Based on the parallel cell finding/analysis strategy and multiple channel techniques, the following throughput estimates were developed. Time estimates for the multiplane image formation and scoring were directly extrapolated from existing program performance at AFRRI and LAI.

System throughput (T_p) is a direct function of the cells scored per patient (C_p), the number of patients (P) and the time to score a single cell (t_s). This total-time requirement is inversely proportional to the number of parallel-analysis channels (C). This relationship is defined in the following equation:

$$T_p = \frac{C_p \text{ x } P \text{ x } t_s}{3600C}$$

The time to score a single cell (t_s) was experimentally determined at between 4 and 10 seconds. This assumes that slide delivery and scoring are performed in a parallel fashion.

Figure 14 presents the throughput in patients scored per hour as a function of the number of channels for 500 patients at three levels of sample size (50, 100,

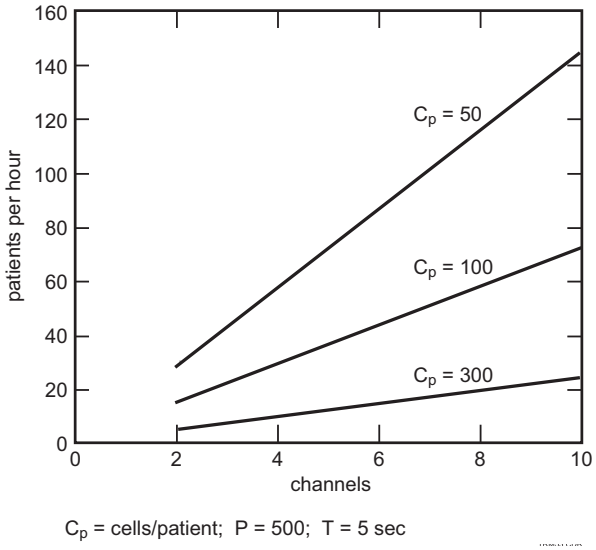

Fig. 14. The effect of multiple scoring channels on the throughput of the cytogenetic halo-comet assay. This graph shows the performance of a multi-channel automated halo-comet assay system. The curves are parametric to the number of cells scored per patient and span the range required by triage and dose assessment. High patient throughput is achieved by increasing the number of analysis channels.

300 cells/patient). These sample sizes span the range of requirements for both the triage and the dose assessment modes of operation. In operational settings, a mixed strategy combining the triage time for the total-patient population with the scoring time for a fraction of the patient population would probably be used.

Table 6 compares the two levels (triage and dose assessment) for three patient-population levels (50, 100, and 500 patients) as a function of the scoring platform size as measured by the number of parallel scoring channels. This table shows that a multiple channel platform with parallel processes can automatically score large patient populations in short analysis times. The system works without human intervention. Image data can also be saved for review on a low-cost computer analysis station.

Conclusions

The proceeding analytical study was performed to investigate the feasibility of fielding an echelon II or echelon III halo-comet cytogenetic scoring system. Under the assumptions detailed in the report, and based on time to score comets and existing hardware capabilities, we conclude that halo-comet and apoptosis assays are viable candidates for a single-use or multiple-use assay platform. Our previous research efforts have shown that a similar conclusion can be drawn for cytogenetic assays employing color-pigmented dicentric, sister-chromated exchange (SCE), and centromere-painted micronucleus assay. All of these assays have relevance to radiation bioassay with the exception of the SCE, which is related to chemical exposure.

In addition to their use in radiation biodosimetry, these assays and their conversion to an automated technique, can play important roles in general medical and clinical assays. Their adoption to general hematologic requirements is relatively straight forward and has been demonstrated in several semi-automated versions.

An added advantage of the systems approach taken here involving proven techniques of microscopic cytogenetics is to provide the capability to do multiple assays on the same hardware. At the same time, the hardware complement used would be identical for both forward-field and rear-support facilities.

Acknowledgments

This research was supported by the Armed Forces Radiobiology Research Institute, Bethesda, MD, under work unit AFRRI-95-3 and CRADA AFRRI/LAI-95. This work was also supported by the National Institutes of Health, National Cancer Institute, Small Business Innovation Research Program Grant No. 1R43 CA72266-01, entitled Automated Non-Fluorescent Chromosome Aberration Scoring. The views expressed are those of the authors; no endorsement by the Armed Forces Radiobiology Institute or the U.S. Department of Defense has been given or should be inferred.

Table 6. The effect of patient population size and C_P on total time requirement.

Number of parallel channels	Time to Score (hours)					
	50 Patients		100 Patients		500 Patients	
	Triage	Dose	Triage	Dose	Triage	Dose
2	1.7	10.4	3.5	20.8	17.4	104.2
4	0.9	5.2	1.7	10.4	8.7	52.1
6	0.6	3.5	1.2	6.9	5.8	34.7
8	0.4	2.6	0.9	5.2	4.3	26.0
10	0.3	2.1	0.7	4.2	3.5	20.8

Triage = 50 cells/patient Dose Assessment = 300 cells/patient t_s = 5 sec

Potential Use of *In Vivo* Electron Paramagnetic Resonance, Electron Spin Resonance (EPR, ESR) for *In Vivo* Dosimetry Under Field Conditions

Harold M. Swartz
Dartmouth Medical School
Hanover, NH

Introduction

The recent development of *in vivo* electron paramagnetic resonance (EPR) techniques, combined with the fact that ionizing radiation generates relatively stable unpaired electron species in hard tissues, makes it feasible to carry out *in vivo* dosimetry with EPR. Such measurements are possible under conditions that will likely be present at forward deployed medical stations.

The occurrence of long-lived radiation induced EPR signals was demonstrated a number of years ago [1]. In hard and/or dry tissues such as bone or teeth these resonances were shown to provide accurate dosimetry at doses as low as 80 rads, even with the equipment available in 1968. It was suggested then that with improvements in techniques and/or the use of other materials, EPR could be used for dosimetry of unplanned exposures from even lower doses of ionizing radiation [2]. Subsequently, EPR technology has developed considerably. In the last few years *in vivo* EPR has been developed and applied successfully to a number of biomedical problems, leading to the likelihood of increased use in human subjects [3].

In addition to direct measurements made *in vivo*, a number of other approaches using EPR dosimetry could provide sensitive and relatively easy measurements of radiation exposure in the field. These include the use of samples which can be removed from subjects (e.g., nail clippings, hair and articles of clothing) and analyzed in highly sensitive instruments. Clothing could be made more sensitive and specific by developing functional uniform components, such as the development of buttons from material with a sensitive and reproducible EPR response to ionizing radiation.

The following sections describe in greater detail EPR's dosimetric potential to obtain useful data under field conditions. It is assumed that under these conditions the most pertinent information would help commanders and medical personnel differentiate between exposures which are 1) insignificant, or 2) significant but unlikely to cause acute symptoms, or 3) likely to result in significant early symptomatology. While it is likely that EPR dosimetry systems could be developed to provide data that are much more precise than this tripartite division for triage, the descriptions in this paper are aimed at achieving quickly the information needed for decision making in the field. It is further assumed that under battlefield conditions, the initial premise will be that significant exposures occur more or less uniformly throughout the body; therefore, dosimetry from any one point or from pooled samples from several sites on the body are sufficient to provide the needed information.

Sites (Samples) To Be Used

On the basis of existing information and results, the most effective site for EPR dosimetric measurements is the teeth. It has already been demonstrated that this tissue has the most sensitive dose-response relationship [2]. The radiation-induced EPR signal in teeth has distinctive characteristics based on its shape and power saturation. The use of teeth also has the advantage of providing a site where good geometry with a sensitive resonator can readily be achieved for entirely non-invasive measurements *in vivo*. It should be possible to place a specially designed resonator around the teeth *in vivo* so that maximum sensitivity is obtained by having the "sample" in the region of highest sensitivity for the resonator; alternatively, a surface type resonator could be used. Because of the relatively low dielectric loss in teeth, it may be possible to use higher frequencies than are ordinarily used for *in vivo* EPR. Although only preliminary results have been reported to date, it seems possible that usable sensitivity could be obtained with the use of fingernail and toenail cuttings. The advantage of these specimens includes the capability to pool samples so that a relatively large mass could be obtained, which could then be measured with a high sensitivity EPR

spectrometer (e.g., 9 GHz, X-band). Additionally, it would be feasible to have an irradiation source available in the field for calibration purposes.

The use of hair has considerations similar to those for toenails and fingernails. In some ways it would be even easier to obtain hair samples in relatively large amounts. The potential disadvantages are the presence of a background signal due to melanin [4] and the potential for loss of signal if the hair is washed [2]. However, it should be feasible to differentiate the EPR signal from melanin on the basis of its line shape and microwave power saturation characteristics. These spectroscopic properties could then be used to implement an automatic method to calculate the signal from melanin and subtract it from the total signal; this would allow the radiation-induced signal from hair to be evaluated accurately.

The use of articles of clothing has advantages similar to those for hair and nails; i.e., these samples could be studied using high sensitivity EPR spectrometers. Perhaps the most attractive aspect involves designing functional articles of clothing such as buttons to serve as emergency dosimeters for assay by EPR. Virtually all solid materials have detectable radiation-induced EPR signals under appropriate conditions. Sensitive and effective dosimetry systems have already been developed based on responses by the amino acid alanine. These systems are now capable of measuring doses well below the requirements for decision-making under field conditions. Although alanine based dosimeters are now widely used, it is clear from a spectroscopic point of view that alanine, because of its complex and wide-line shape, is far from an ideal EPR dosimeter. However, it should be relatively straightforward to find plastic materials with better suited radiation-induced stable EPR lines. Such materials could be incorporated into uniform parts, such as buttons.

Instrumental Aspects

Direct *in vivo* EPR usually requires the use of EPR instruments which operate at lower frequencies, such as 1 Ghz [3]. This is because large amounts of materials, especially water, which non-resonantly absorb the frequencies used for conventional EPR spectroscopy (9 GHz), are present in tissues. While *in vivo* EPR spectroscopy has been developing rapidly and is being used increasingly for many studies, it does have significantly less sensitivity than EPR spectroscopy which uses conventional higher frequencies. Teeth, however, are an exception to the general rule that tissues are composed of 70% to 90% water; therefore, the sensitivity of EPR for studies of teeth should be higher than for most tissues. Precise data on these differences are not available presently but could be readily obtained in days or weeks.

Such studies would then facilitate the decision as to the appropriate instrumental conditions to use for EPR dosimetry under field conditions. Key variables to consider are the amount of incident microwave power that can be used effectively for studies within the mouth, and the resulting signal to noise ratio. These factors, in turn, would be affected by the choice of frequency and the type of resonant structure that is employed. The frequency and strength of the modulation would be another important factor to optimize. In general, one would aim to use the highest practical frequency to make measurements with teeth under *in vivo* conditions. If it is determined that a frequency higher than 1 GHz would be applicable for study of teeth *in vivo*, the principles that already have been implemented for the construction of *in vivo* EPR instruments at 1 GHz could be utilized.

The implementation of a system to use *in vivo* EPR to make measurements of radiation exposure under field conditions seems relatively straightforward. Although the following is based on our experience in developing *in vivo* EPR at 1.2 GHz, the approach is similar for most applicable frequencies. The engineering of a system that could be operated in the field for this special use should present no particular difficulties. The construction of the microwave bridge and control system can be designed for rugged use and portability. The controls and output can be configured, using a portable computer, so that an operator with minimal technical background can obtain an unambiguous result in the form of a number that indicates the extent of radiation exposure. The power requirements for this part of the spectrometer are modest.

The strength and configuration of the magnetic field would depend on the choice of spectrometer operating frequency. If a lower frequency spectrometer is chosen, then either a large magnet in which the subject would be positioned between the magnetic poles could be used; or, a structure could be developed in which a small magnetic field of appropriate strength is generated at the site where the measurements will be made. The latter configuration would be the likely method of choice if a higher frequency EPR spectrometer will be used; this would keep the size of the instrument suitable for field use. We recently carried out a detailed feasibility study for a fully portable instrument at 1 GHz, using a magnet system into which the subject was placed. We tested some of the critical components and did not find any crucial limitations.

The choice of resonator is important, but could be made from among those which have been developed and are already in use. The previously described coupled circuit with a loop is the most likely resonator configuration [3]. Such a resonator could be constructed to allow the loop to be placed around the tooth to be measured. This would provide the best geometric condition for achieving an optimum signal to noise ratio. Alternatively, a surface resonator [5], which could be shaped to fit the contours of teeth, could be used. There might be some advantages in using a dielectric resonator [6]. The use of a frequency of 1.1 GHz would be the simplest system to implement quickly. To maximize sensitivity, serious consideration should be given to systems that operate at higher frequencies.

A conventional EPR instrument could be used on samples that are removed from the subject (e.g., nail clippings, or articles of clothing). The sample would be placed at an optimum position within a fixed magnet system. Such an instrument also could be developed for dual use, to measure *in vitro* objects of clothing, etc., which might have even more readily detectable radiation-induced EPR signals [2].

Any of the instruments described above could be designed to be operated by minimally trained personnel and could be used for screening large numbers of people. At least initially under these circumstances the results would be semi-quantitative, and would be sufficient to provide firm guidance for decision making in the field. Such an instrument could be designed to indicate a radiation dose within the precision needed for the purpose.

References

1. Swartz HM (1965) Long-lived electron spin resonances in rats irradiated at room temperature. Radiation Res 24:579-586

2. Brady JM, Aarestad NO, Swartz HM (1968) *In vivo* dosimetry by electron spin resonance spectroscopy. Health Physics 15:43-47

3. Swartz HM, Bacic G, Gallez B, Goda F, James P, Jiang J, Liu KJ, Mader K, Nakashima T, O'Hara J, Shima T, Walczak T (1995) *In vivo* EPR spectroscopy. In: Ohya-Nishiguchi H, and Packers L (eds) Bioradicals detected by ESR spectroscopy. Birkhauser Verlag, Basel, Switzerland, 285-299

4. Enochs WS, Nilges MJ, Swartz HM (1993) A standardized test for the identification and characterization of melanins using electron paramagnetic resonance (EPR) spectroscopy. Pigment Cell Biology 6:91-99

5. Nilges MJ, Walczak T, Swartz HM (1989) 1 GHz *in vivo* ESR spectrometer operating with a surface probe. Phys Med 5:195-201

6. Jiang J, Liu KJ, Swartz HM (1996) Low frequency EPR surface probe based on dielectric resonator. Chemical Intermediates, 22: 539-547

EPR-Based Dosimetry and Its Present Suitability for Field Usage

Arthur H. Heiss
Bruker Instruments, Inc.
Billerica, MA

The recent development of a small and relatively portable EPR analyzer with nearly the sensitivity of a research instrument opens the possibility of bringing EPR measurements to the field [1].

Electron Paramagnetic Resonance has long been accepted as an accurate and reliable method for the qualitative and quantitative determination of the effects of ionizing radiation. Work to date has been performed on research instruments which, due to their size and weight, are confined to a laboratory environment. The EMS 104 EPR Analyzer (Fig.15.) is small by comparison and requires neither cooling water nor three-phase power, making it suitable for field use. Development of a practical computerized control system also provides quantitative measurements with minimal operator training. Appropriate software has been developed for assays using several distinctly different dosimetry systems.

Electron Paramagnetic Resonance (EPR)

Unpaired electrons are created by ionizing radiation; and their presence can be used to measure the radiation dose administered to a suitable sample. Electron Paramagnetic Resonance is a form of spectroscopy that observes unpaired electrons in various substances by stimulating transitions between normally degenerate Zeeman energy levels separated by the application of an external magnetic field. The EPR Spectrometer consists of a magnet system capable of producing the required field, typically .35T, and suitable field sweep capability to display the spectral region of interest. The sample is placed in a microwave rf field whose frequency corresponds to the separation in Zeeman levels caused by the external field, typically 10 GHz. The absorption of energy by the sample is then plotted as a function of field. Computerization of the instrument allows automatic acquisition of the signal and computation of the applied dose. A block diagram of the EMS 104 is shown in Fig. 16.

Alanine

Crystalline alanine when subjected to ionizing radiation is converted predominantly to a stable paramagnetic species, CH_3-C*H-COOH. The 5-line EPR spectrum is well characterized and the amplitude of the central line is proportional to applied dose. Thus, the use of alanine pellets and films for dosimetry in radiation processing provides the ease and convenience of a long-lived, cumulative, rereadable dosimeter that can be attached to products or carried by personnel [2]. These dosimeters can be packaged and labeled for easy identification and read using automated equipment; doses are displayed directly in Gray by the instrument. Alanine

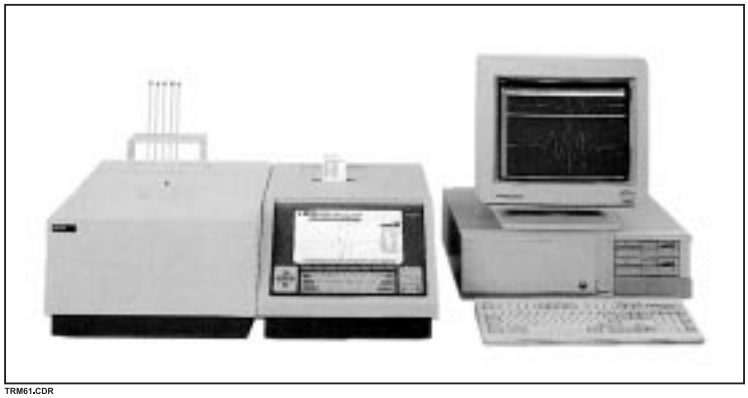

TRM61.CDR

Fig. 15. The EMS 104 EPR Analyzer requires neither cooling water nor three-phase power—suitable for field use.

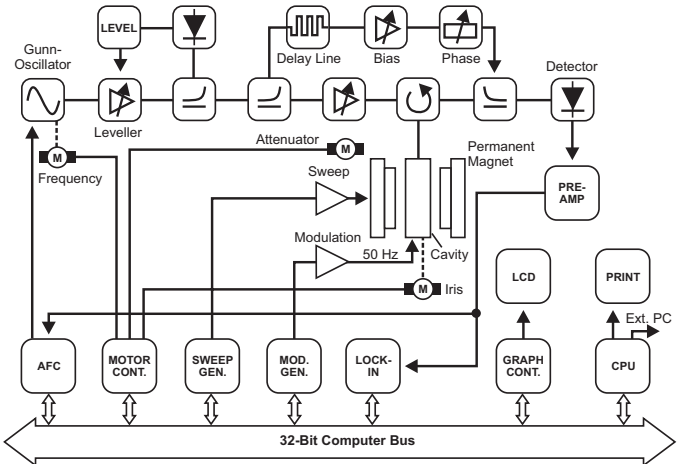

Fig. 16. A block diagram of the EMS 104.

is currently well established as a transfer standard dosimeter in the radiation processing community; and an ASTM standard (E 1607) exists detailing procedures and usage of alanine pellets.

The useful range of alanine pellets, typically 5mm diameter x 5mm height, is from ca. 1 Gy to 10^5 Gy using commercially available pellets. This range can be extended to lower dose levels by increasing the size of the sample and the measurement time; although measurements below 0.1 Gy are difficult. Alanine films are also commercially available. Being flexible, they may be incorporated in or attached to clothing or other sheet materials. However, with a lower mass, they have higher minimum detectable dose levels.

Alanine dosimeters have been shown to be independent of dose rate. They are suitable for beta, x-ray, and gamma radiation, and have a minimal temperature dependence and linear response up to tens of kilograys with excellent polynomial fits at higher doses. Readout for doses greater than a few gray can be performed in seconds with high confidence levels. A typical segment of the alanine-derived radical spectrum (the central line of a five-line spectrum) used for analysis is shown in Fig. 17; and a typical calibration curve is shown in Fig. 18.

Spin Label Assays

The development of spin-label assays for radiation dose using whole blood provides another possibility for field use of EPR. The preparation of a suitable sample requires only a few minutes; and the sample can be read in seconds. Spin labels do not have adverse problems associated with radioisotopes and can be stored indefinitely. Changes in receptor-binding properties of human red blood

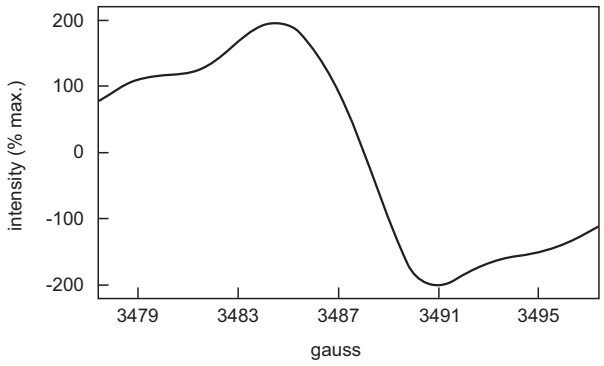

Fig. 17. A typical segment of the alanine-derived radical spectrum (the central line of a five-line spectrum) used for analysis.

Fig. 18. Typical calibration curve for alanine dosimeters.

cells have been studied at the membrane level using spin labeled insulin. Preliminary studies made at the Armed Forces Radiobiology Research Institute (AFRRI) have shown a distinct and measurable difference in the number of binding sites measured between the unirradiated and irradiated cells. Further work is needed to better characterize the effect and determine dose vs. binding curves. However, this method shows promise both as a means of determining levels of irradiation applied to blood used for transfusion and blood drawn from accident victims.

Tooth and Bone

The use of bone samples is also well established for determining exposure to ionizing radiation and is an established method in Europe where irradiation of foodstuffs is prohibited in certain markets. The major problem with bone measurements is the uncertainty in determining the background, as well as the wide variation in sample density [3]. EPR measurements to determine dose in bone usually require the exposure of the sample to additional radiation to establish a dose-response curve. Back-extrapolation is then used to determine the initial dose. This is easily accomplished in the laboratory but would be unsuitable for a field measurement.

Since tooth enamel contains 95–98% hydroxyapatite it is more suitable for field use in dosimetry than bone; as enamel is more uniform and contains fewer impurities. Considerable research has been done in determining dose using EPR measurements on extracted teeth. Ikeya and others have done extensive work on the teeth of A-bomb survivors and developed suitable dosimetry methods [4].

Some developmental work has been done on EPR measurements of unextracted incisors using portable magnets and a surface probe. The higher sensitivity of the EMS 104 and its modular nature make it adaptable to incorporating such a probe as an extension to the existing instrument. The use of the EMS 104 electronics in combination with an MRI magnet's fringe field would considerably lessen the difficulties of bringing this technique forward, as in the case of screening accident victims. The growing availability of MRI systems in most populated areas makes this a reasonable consideration. The experimental problem is reduced from having to produce the main external field to producing only the field sweep and modulation; a task that is made considerably less difficult by utilizing existing EMS 104 electronics.

In addition, work on shell buttons has shown significant sensitivity in the concentration of CO_2 to ionizing radiation in the 0–10 Gy range. Spectra similar to those obtained from fossil shells are obtained; and results consistent with other dosimeters are found. Distribution of buttons of suitable inorganic or polymer materials would be innocuous. These could be attached to clothing and read following exposure with few problems. Determining background dose would cease to be a problem as this could be determined for an entire batch beforehand in the laboratory.

Bruker Instruments, Inc. has developed several instruments for military field use, including the MM-1, the first mil-spec fully mobile chemical warfare agent mass spectrometer for military warfare agent detection, and is currently testing, under a current government contract, a Bruker developed mass spectrometer with bio-agent detection for use on a battlefield with chemical contaminants. As a result, the extension of these efforts to produce a rugged, portable EPR spectrometer is well within the capability and scope of the company's manufacturing facilities in the United States and Europe. It remains to be seen if sufficient demand for such an instrument exists to prompt further development.

References

1. Maier D, Schmalbein D (1993) A dedicated EPR analyzer for dosimetry. Int J Appl Radiat. Isot. 44:345-350.

2. ASTM (1995) Standard practice for use of the alanine-EPR dosimetry system. In Annual book of ASTM standards, Section 12, Volume 12.02: E 1607-94.

3. McLaughlin WL (1993) ESR dosimetry. Proceedings of 10th International Conference on Solid State Dosimetry. Radiat Prot Dosimetry

4. Ikeya M (1993) New applications of electron spin resonance: dating, dosimetry and microscopy. World Scientific Publishing Co., River Edge, NJ